Published in final edited form as:
New Phytol. 2014 September ; 203(4): 1128–1145. doi:10.1111/nph.12911.

Transcriptomic and physiological characterization of the *fefe* mutant of melon (*Cucumis melo*) reveals new aspects of iron–copper crosstalk

Brian M. Waters, **Samuel A. McInturf**, and **Keenan Amundsen**
Department of Agronomy and Horticulture, University of Nebraska, Lincoln, NE 68583-0915, USA

Summary

- Iron (Fe) and copper (Cu) homeostasis are tightly linked across biology. In previous work, Fe deficiency interacted with Cu regulated genes and stimulated Cu accumulation.
- The C940-fe (*fefe*) Fe uptake mutant of melon (*Cucumis melo*) was characterized, and the *fefe* mutant was used to test whether Cu deficiency could stimulate Fe uptake. Wild type and *fefe* mutant transcriptomes were determined by RNA-seq under Fe and Cu deficiency.
- *FeFe* regulated genes included core Fe uptake, metal homeostasis, and transcription factor genes. Numerous genes were regulated by both Fe and Cu. The *fefe* mutant was rescued by high Fe or by Cu deficiency, which stimulated ferric-chelate reductase activity, *FRO2* expression, and Fe accumulation. Accumulation of Fe in Cu deficient plants was independent of the normal Fe uptake system. One of the four *FRO* genes in the melon and cucumber (*Cucumis sativus*) genomes was Fe regulated, and one was Cu regulated. Simultaneous Fe and Cu deficiency synergistically upregulated Fe uptake gene expression.
- Overlap in Fe and Cu deficiency transcriptomes highlights the importance of Fe– Cu crosstalk in metal homeostasis. The *fefe* gene is not orthologous to *FIT*, thus identification of this gene will provide clues to help understand regulation of Fe uptake in plants.

Keywords

copper (Cu); ferric-chelate reductase; *fefe* mutant; iron (Fe); iron–copper crosstalk; melon (*Cucumis melo*); metal homeostasis

Author for correspondence: *Brian M. Waters Tel: +1 402 472 0153*bwaters2@unl.edu.

Supporting Information Additional supporting information may be found in the online version of this article.

Please note: Wiley Blackwell are not responsible for the content or functionality of any supporting information supplied by the authors. Any queries (other than missing material) should be directed to the *New Phytologist* Central Office.

Introduction

Iron (Fe) and copper (Cu) are trace metals that are required by plants for their roles in redox metabolism, such as mitochondrial respiration, photosynthesis, and nitrogen fixation (Puig *et al.*, 2007; Burkhead *et al.*, 2009; Hansch & Mendel, 2009; Pilon *et al.*, 2011). Excess Fe or Cu leads to oxidative stress and damage from reactive oxygen species (Halliwell & Gutteridge, 1992). However, Fe and Cu are both involved in protection from reactive oxygen species (Hansch & Mendel, 2009) as components of peroxidases, catalase, and superoxide dismutases (SODs). Iron-containing SODs (FeSODs) and Cu-containing SODs (CuSODs) are functionally interchangeable, but are products of different genes (Kliebenstein *et al.*, 1998; Alscher *et al.*, 2002; Myouga *et al.*, 2008; Pilon *et al.*, 2011).

Iron deficiency responses include increased expression of certain genes to increase Fe uptake and to make cellular adjustments to maintain homeostasis. The bHLH transcription factor *FIT* is required for normal regulation of Fe uptake genes in Arabidopsis (Colangelo & Guerinot, 2004; Jakoby *et al.*, 2004), including the ferricchelate reductase *FRO2*, the primary Fe transporter *IRT1*, and another Fe transporter, *NRAMP1*. The FIT protein interacts with other Fe regulated bHLH proteins, such as bHLH100, bHLH101, bHLH038, and bHLH039 (Yuan *et al.*, 2008; Wang *et al.*, 2013), and these proteins also have regulatory roles independent of FIT (Sivitz *et al.*, 2012; Wang *et al.*, 2013). Several metal homeostasis genes respond to both Fe and Cu, such as the metal transporters *COPT2* and *ZIP2*, and the ferric-chelate reductase *FRO3* (Sancenon *et al.*, 2003; Wintz *et al.*, 2003; Colangelo & Guerinot, 2004; Mukherjee *et al.*, 2006; Buckhout *et al.*, 2009; del Pozo *et al.*, 2010; Garcia *et al.*, 2010; Yang *et al.*, 2010; Stein & Waters, 2012; Waters *et al.*, 2012). Similarly, Cu deficiency results in upregulated ferric-chelate reductase activity in roots (Norvell *et al.*, 1993; Welch *et al.*, 1993; Cohen *et al.*, 1997; Romera *et al.*, 2003; Chen *et al.*, 2004). Arabidopsis *FRO4* and *FRO5* are upregulated by Cu deficiency but not by Fe deficiency (Bernal *et al.*, 2012), and provide low-level but significant ferric-chelate reductase activity.

Changes in availability of one mineral nutrient often results in changes in homeostasis of other minerals. For example, Fe deficiency caused changes in expression of genes related to potassium and phosphate (Wang *et al.*, 2002) and sulfate (Paolacci *et al.*, 2013) homeostasis. Fe homeostasis interacts with Zn tolerance (Pineau *et al.*, 2012), and Cu deficiency interacts with phosphate signaling (Perea-García *et al.*, 2013) and cadmium tolerance (Gayomba *et al.*, 2013). Copper concentration was higher in Fe deficient leaves (Welch *et al.*, 1993; Chaignon *et al.*, 2002; Waters *et al.*, 2012; Waters & Troupe, 2012). Several Cu responsive genes and microRNAs had altered abundance under Fe deficiency in *Arabidopsis thaliana* (Stein & Waters, 2012; Waters *et al.*, 2012). This suggested that a specific role for accumulation of Cu under Fe deficiency is the replacement of FeSOD, which decreases under Fe deficiency (Kurepa *et al.*, 1997; Waters *et al.*, 2012), with CuSOD, whose transcripts increase in Fe deficient leaves (Waters *et al.*, 2012). Supporting this hypothesis, counteraction of oxidative stress was impaired when formation of functional CuSOD protein was blocked under Fe deficiency (Waters *et al.*, 2012). Increasing evidence points to the importance of Fe–Cu crosstalk in metal homeostasis (Bernal *et al.*, 2012; Waters *et al.*, 2012; Perea-García *et al.*, 2013).

Mutant lines with altered metal homeostasis are valuable tools to study molecular and physiological responses to metal stress. The *fefe* mutation originated spontaneously in the melon (*Cucumis melo*) variety Edisto, and was crossed into the variety Mainstream to generate the C940-fe germplasm (Nugent & Bhella, 1988; Nugent, 1994). The *fefe* mutant lacks ferric-chelate reductase activity and rhizosphere acidification (Jolley *et al.*, 1991), two of the important mechanisms of the reductive strategy of Fe uptake in dicots and non-grass monocots. The *fefe* mutant has chlorotic leaves typical of Fe deficiency, which can be corrected by application of external Fe. These signs point to *fefe* as a regulator of Fe uptake, but the mutant was not fully physiologically characterized to determine if the mutation is specific to root function. Additionally, gene expression levels in *fefe* had not been characterized.

Our overall objective in this study was to use the *fefe* mutant to increase understanding of Fe uptake regulation and to explore Fe–Cu crosstalk through characterization of transcriptomes of Fe and Cu deficient plants. Our specific goals were to: physiologically characterize the *fefe* mutant; use the *fefe* mutant to test whether Cu deficiency can interact with the Fe regulatory pathway to stimulate Fe accumulation; and determine transcriptomes in wild type (WT) and *fefe* plants in control and Fe or Cu deficient conditions to identify genes that are regulated by one or both metals. Here, we show that the *fefe* defect caused loss of normal regulation of Fe accumulation, was specific to roots, and could be rescued by Cu deficiency, which stimulated Fe uptake. Furthermore, we uncovered new synergistic interactions between Fe and Cu deficiencies on Fe uptake processes.

Materials and Methods

Plant growth and materials

Seeds were purchased for cucumber (*Cucumis sativus* L.) cv Ashley (Jung Seed Co., Randolph, WI, USA) and melon (*Cucumis melo* L.) cv Edisto (Victory Seed Company, Molalla, OR, USA). Seeds of ‘snake melon’ (PI 435288) were obtained from the USDA National Plant Germplasm System. Seeds of C940-fe (*fefe*) melon (Nugent, 1994) were a generous gift from Michael A. Grusak, USDA-ARS Children’s Nutrition Research Center, Houston, TX, USA.

Plants were grown in a continuously aerated nutrient solution with the following composition: 0.8 mM KNO_3, 0.4 mM $Ca(NO_3)_2$, 0.3 mM $NH_4H_2PO_4$, 0.2 mM $MgSO_4$, 20 μM Fe(III)-EDDHA (Sprint 138, Becker-Underwood, Ames, IA, USA), 25 μM $CaCl_2$, 25 μM H_3BO_3, 2 μM $MnCl_2$, 2 μM $ZnSO_4$, 0.5 μM $CuSO_4$, 0.5 μM Na_2MoO_4 and 1 mM MES buffer (pH 5.5) or, if indicated, HEPES buffer (pH 7.1). Fe was omitted or supplied as indicated for Fe supply treatments, and Cu was omitted or supplied as indicated for Cu supply treatments. For N source experiments, the same micronutrients described above were used, with a macronutrient solution of: 0.7 mM K_2SO_4, 0.1 mM KH_2PO_4, 0.1 mM KCl, 0.5 mM $MgSO_4$, and 1 mM $CaCl_2$. Nitrogen was added at a final concentration of 2.5 mM as $(NH_4)_2SO_4$ or KNO_3.

Melon and cucumber seeds were sprouted on germination paper in a 30°C incubator until transplanting to hydroponics after 4 d. Seedlings were placed in sponge holders in lids of

black plastic containers, 4 plants per 750 ml solution. Plants were grown in a growth chamber with a mix of incandescent and fluorescent light at 300 μmol m^{-2} s^{-1}. For cucumber, plants were pretreated in standard solution for 5 d before nutrient treatments for 3 d. For the -Cu *fefe* mutant rescue and WT controls, seedlings were grown without Cu from initial planting for 9 d. Plants for the +/- Cu RNA-seq experiment (Edisto and *fefe*) were collected at 9 d. For the +/- Fe RNA-seq experiment, wild-type (Edisto and snake melon) and *fefe* mutants were pretreated for 9 d on -Cu solution, and only *fefe* mutants that had green leaves were used for treatments of 3 d duration. The purpose for the -Cu pretreatment was to use only healthy *fefe* plants so that the transcriptome would reflect the Fe regulated genes in *fefe* rather than secondary effects of severe Fe deficiency.

For grafting experiments, melon seeds were germinated and planted as described above. After 2 d growth in the growth chamber in complete nutrient solution, seedlings were removed from sponge holders and stems were cut at an angle above the crown. Root stocks and scions were joined with a silicon grafting clip, plants were returned to hydroponics containers, and placed in a high humidity chamber under dimmed lighting (150 μmol m^{-2} s^{-1}) for 7 d while the grafted tissues fused. Plants were then moved to a growth chamber for 3 d before Fe treatments were applied for 3 d. To avoid potential variation resulting from the circadian clock, sampling for ferric-chelate reductase activity or RNA was always performed between the hours of 14:00 and 16:00.

Ferric-chelate reductase activity

Root ferric reductase assays were performed for 30–60 min on individual roots, using 30 ml of an assay solution of 0.1 mM ferrozine (3-(2-Pyridyl)-5,6-diphenyl-1,2,4-triazine-4′,4′-disulfonic acid sodium salt, Sigma-Aldrich, St Louis, MO, USA), 0.1 mM Fe(III)-EDTA and 1 mM MES buffer (pH 5.5) (Fisher Scientific, Fair Lawn, NJ, USA). Reduced Fe was calculated using absorbance at 562 nm using the extinction coefficient 28.6 mM^{-1} cm^{-1}.

Mineral analysis

Iron and Cu concentrations were determined by ICP-MS as described previously (Waters & Troupe, 2012). To calculate total mineral quantity in each plant part and the sum of all parts, Fe and Cu contents were calculated by multiplying concentration by organ DW. Briefly, plant tissues were dried for at least 48 h at 60°C in a drying oven. Tissues were weighed and digested overnight at room temperature in 3 ml concentrated HNO_3. Samples were then heated at 100°C for 2 h, followed by addition of 3 ml H_2O_2, then heated stepwise to 165°C until dryness. Residues were resuspended in 5 ml 1% HNO_3 before ICP-MS.

cDNA identification

Primers for full-length cucumber *IRT1* (Waters *et al.*, 2007) were used with melon cDNA as a template to amplify a PCR product that was cloned and sequenced. The melon cDNA was 96% identical to cucumber *IRT1*. This transcript was Fe regulated as expected and was designated *CmIRT1*. A full-length ferric reductase cDNA was identified from Fe deficient roots by a degenerate primer RACE PCR strategy as described previously (Waters *et al.*, 2002) and designated *CmFRO1*. Following release of the cucumber genome, three additional *FRO* genes were identified by BLAST; *FRO2*, Cucsa.108040.1; *FRO4*, Cucsa.260380.1

(http://www.phytozome.net), and *FRO3*, Csa008439 (http://www.icugi.org). Of these melon *FRO* genes, *FRO1* is the ortholog of Arabidopsis *FRO2*. A *FIT* homolog (Csa015217) was identified by a BLAST search against the cucumber genome, version 1 (http://www.icugi.org/cgibin/ICuGI/genome/home.cgi?ver=1&organism=cucumber). Primers designed to amplify the full cDNA also amplified a single cDNA from melon, which was 97% identical at the nucleotide level and was Fe regulated, and was designated *CmFIT*.

Real time RT-PCR

Total RNA was extracted from roots using the Plant RNeasy kit (Qiagen, Hilden, Germany). RNA quality and concentration was determined by UV spectrophotometry. 1 μg of DNase-treated RNA (RNase-free DNase I, New England Biolabs, Ipswich, MA, USA) was used for cDNA synthesis, using the High Capacity cDNA Reverse Transcription kit (ABI, Foster City, CA, USA) with random hexamers at 2.5 μM final concentration. cDNA corresponding to 1.5–2.5 ng of total RNA was used in a 15 μl real-time PCR reaction performed in a MyIQ (Bio-Rad, Hercules, CA, USA) thermal cycler using GoTaq qPCR MasterMix (Promega, Madison, WI, USA) and 0.2 μM gene-specific primers (Supporting Information Table S1). The following standard thermal profile was used for all PCRs: 50°C for 2 min, 95°C for 8 min; 40 cycles of 95°C for 15 s, 56°C or 65°C for 15 s, and 72°C for 15 s. The C*t* values for all genes were calculated using BioRad IQ5 System Software version 2.0 (BioRAD, Hercules, CA, USA). Gene expression was determined by normalizing to the C*t* value of ubiquitin using the Livak method (Livak & Schmittgen, 2001), with the equation Relative Expression= $2^{-\Delta\Delta Ct}$, where $\Delta\Delta Ct$ = ($Ct_{target\ gene}$ (treatment 1) - $Ct_{target\ gene}$ (control treatment)) - (Ct_{UBQ} (treatment 1) - Ct_{UBQ} (control treatment)).

Next Generation Sequencing and bioinformatics

Sources of RNA samples were described above. RNA-seq was performed using an Illumina HiSeq 2000 instrument. Barcoded libraries were constructed from 3 μg of root total RNA, with three biological replicate libraries per treatment. Replicates were run in separate lanes, with a total of six samples from different treatments in each lane. The reads are available as NCBI BioProject: PRJNA244361 (http://www.ncbi.nlm.nih.gov/bioproject/244361). Because there is high synteny between melon and cucumber, and orthologues of these species are highly co-linear within large segments of chromosomes (Huang *et al.*, 2009; González *et al.*, 2010), the cucumber transcriptome was used as the reference for read mapping. The cucumber transcriptome sequence reference (cucumber_v2.cds.gz) was obtained from the cucurbit genomics database (ftp://www.icugi.org/pub/genome/cucumber/v2/). Sequencing reads from each sample were mapped to the reference database using BOWTIE2 (Langmead & Salzberg, 2012) with --local -N 1 options and cleaving 15 bp from each end of the reads. The BOWTIE2 output bam files were converted to sam format using SAMtools (Li *et al.*, 2009). Perl scripts were written to extract read counts from the sam files and to create a read count data matrix. The data matrix was imported into R and analyzed using the Bioconductor package edgeR (Robinson *et al.*, 2010). Read counts in each library were normalized to account for the library size using the calcNormFactors function, and tag-wise dispersions were estimated by using an empirical Bayes estimate, which is dependent on the initial dispersion estimates, through the estimateGLMTagwiseDisp and estimateGLMTrendedDisp functions, respectively.

Differential expression was called for genes with an FDR moderated q-value (Benjamini & Hochberg, 1995) less than 0.05, and also showed a 1.0 log fold change in expression and greater than 20 reads in at least one treatment.

Results

Physiological characterization the *fefe* mutant

When grown in standard nutrient solution, *fefe* cotyledons are green, but the first true leaf is chlorotic. We first corroborated previous reports (Nugent & Bhella, 1988; Nugent, 1994) that additional Fe supply could reverse leaf chlorosis. When three to five 2 μl droplets of 5 mM Fe(III)-EDDHA were applied to the second true leaf, that leaf and the emerging third true leaf had become green 36 h later (Fig. S1). Other forms of Fe also led to re-greening of *fefe* leaves, including ferric-EDTA, ferric citrate, ferric ammonium sulfate, and ferric nitrate, demonstrating that additional Fe was sufficient for reversal of the phenotype. A second test was to increase Fe availability in hydroponics by manipulating the nutrient solution in two ways. First, we used MES or HEPES buffer to maintain the solution at pH 5.0 or 7.1, respectively, while supplying either 1 μM or 20 μM Fe. In the WT these treatments had no discernible effect on leaf color (Fig. S1). The first leaf of *fefe* was chlorotic in all treatments except the low pH and high Fe combination. A second manipulation of the nutrient solution was to grow plants with either nitrate (NO^-_3) or ammonium (NH^+_4) as the sole N source. On NO^-_3, *fefe* plants had the usual chlorotic first leaf, whereas on NH^+_4, the first true leaf was green. Uptake of NH^+_4 uses a H^+ antiport mechanism (von Wiren *et al.*, 2000), resulting in net efflux of H^+ into the nutrient solution, which in this case lowered the pH to below 4.0 and shifted Fe to the more readily available ferrous form. These manipulations support the idea that the defect in *fefe* is specific to Fe uptake.

In previous work we showed that cucumber cotyledons grow (e.g. increase in DW) and accumulate Fe and certain other minerals over the first few days after germination (Waters & Troupe, 2012). To test whether *fefe* accumulated Fe or utilized Fe stored in cotyledons, we measured DW and Fe content of cotyledons in WT and the *fefe* mutant (Fig. 1). Cotyledons of *fefe* at germination were of similar size to WT (Fig. 1a), and had slightly less Fe content (Fig. 1b). Cotyledons of *fefe* grew similarly to those of WT, as evidenced by increased DW from germination to 6 d later. However, WT cotyledons gained over 5 μg of Fe, while *fefe* cotyledons did not gain significant amounts of Fe, nor did they decrease in Fe, demonstrating that *fefe* seedlings did not accumulate Fe from the nutrient solution during early growth.

To corroborate previous reports that *fefe* roots do not induce ferric-chelate reductase activity, mutant and WT plants were grown on a range of Fe concentrations. WT roots had high ferric-chelate reductase activity at low Fe supply, but *fefe* had low activity at all Fe concentrations (Fig. 2a), demonstrating that inducible ferric-chelate reductase activity is diminished in *fefe*. However, on some occasions ferric-chelate reductase activity was somewhat elevated in *fefe* (e.g. Expt 2, 10 μM), which indicated that the ferric-chelate reductase protein is functional, but is not properly regulated. This led to the question of whether the *fefe* defect is specific to ferric reductase, or if other Fe uptake components are not expressed normally. To address this, we identified orthologs of Arabidopsis *FRO2*,

IRT1, *Nramp1*, and *FIT* in melon and designed primers to measure transcript abundance by real-time RT-PCR. These genes were upregulated in low Fe conditions in WT, but not in *fefe* (Fig. 2b), suggesting that the *fefe* defect could be in the *FIT* gene, since melon FIT should regulate melon *FRO1* (the Arabidopsis *FRO2* ortholog) and *IRT1* as in Arabidopsis and tomato (Ling *et al.*, 2002; Colangelo & Guerinot, 2004). Sequencing of *FRO1* and *IRT1* cDNAs, and genomic DNA of *FIT* in both WT and *fefe* mutants did not reveal any polymorphisms that would result in premature stop codons or frame shifts, or amino acid changes that would be expected to abolish protein function, suggesting that the *fefe* gene is a regulator of Fe uptake that acts upstream of the primary Fe uptake genes and the *FIT* transcription factor.

As further characterization of the *fefe* mutant, we determined whether the defect was localized to roots or shoots. Reciprocal grafting was conducted with *fefe* and the parental wild type Edisto roots or shoots, and as controls each genotype was grafted to itself. Grafted plants with *fefe* roots were chlorotic, with either *fefe* or Edisto shoots, whereas *fefe* shoots were of a normal green color if grafted to WT rootstock (Fig. 3). Also, *fefe* roots of these plants did not induce ferric-chelate reductase activity regardless of shoot genotype. These results indicate that the *fefe* defect is in a regulatory component of the root system, and could result from an inability to receive a signal from the shoots, or from a signal transduction defect resulting in failure to respond and activate physiological and gene expression responses.

Can Cu deficiency stimulate Fe accumulation?

Since low Fe supply caused plants to accumulate additional Cu in leaves (Welch *et al.*, 1993; Chaignon *et al.*, 2002; Waters *et al.*, 2012; Waters & Troupe, 2012), we hypothesized that under low Cu supply there would be a higher demand for Fe, which should lead to increased Fe uptake and rescue the *fefe* phenotype. This hypothesis was correct, as *fefe* plants grown without Cu (+Fe, −Cu) recovered within 9 d and had a green first leaf phenotype, while plants grown on complete solution (+Fe, +Cu) had the typical yellow first leaf (Fig. 4a). We then asked whether ferric-chelate reductase activity was increased in the *fefe* plants under Cu deficiency. When rescued *fefe* plants (green first leaf) were transferred to −Fe−Cu or −Fe+Cu treatments for 3 d, an approx.. 3-fold increase in root ferric-chelate reductase activity was observed in the -Cu treatment (Fig. 4b), although total activity was substantially lower than typically seen in WT Fe deficient roots. We also dissected *fefe* and WT plants grown with or without Cu for 12 d for mineral content analysis to determine the total quantity of Fe and Cu in the plants. The biomass of the plant parts showed that *fefe* affected growth of the first leaf primarily (Fig. 4c). On -Cu treatments, Cu content (Fig. 4d) was similar in both genotypes, and lower than plants on the +Cu treatment. In control solution, the total plant Cu content was lower in *fefe* than WT, primarily resulting from smaller leaves. There was no difference in Cu content between *fefe* and WT in the -Cu treatment. Total Fe content was much lower in *fefe* plants grown in complete solution, and this was most pronounced in leaves (Fig. 4e). The *fefe* and WT plants had a similar total quantity of Fe when Cu was withheld and *fefe* had recovered, demonstrating that Fe accumulation was stimulated by Cu deficiency. WT plants also accumulated more Fe under -Cu then +Cu conditions (Fig. 4e), even though DW was similar (Fig. 4c). Thus, the

stimulation of Fe accumulation by Cu deficiency in the whole plant, which by definition would require increased uptake, occurred in both WT and *fefe* mutant plants.

Because both WT and *fefe* plants accumulated additional Fe under Cu deficiency, and Cu deficient *fefe* plants had increased ferric-chelate reductase activity (Fig. 4), we determined which *FRO* gene(s) responded to each metal. We first addressed this question in cucumber since the cucumber and melon genomes are highly homologous (Huang *et al.*, 2009; González *et al.*, 2010), and the cucumber genome has been sequenced (Huang *et al.*, 2009) and annotated. Plants were treated with complete or -Fe solutions with a range of Cu concentrations, because ferric-chelate reductase activity is sensitive to Cu supply (Waters & Armbrust, 2013). Root reductase activity was highest in -Fe-Cu roots, and was slightly lower as Cu was supplied at 0.25 and 0.5 μM (Fig. 5a). Expression of *FRO1*, the primary ferric-chelate reductase (Waters *et al.*, 2007), was elevated at 0, 0.25, and 0.5 μM Cu (Fig. 5b). Ferric-chelate reductase activity decreased as Cu supply increased, and did not tightly correspond to *FRO1* expression, which did not decrease at 0.5 μM Cu. However, at 2.0 μM Cu, both root ferric-chelate reductase activity and *FRO1* expression were abolished, and had lower values than those of control (+Fe, 0.5 μM Cu) roots. The -Fe 2.0 μM Cu treated roots may have been suffering from Cu toxicity, as Cu is toxic at lower levels in Fe deficient roots (Waters & Armbrust, 2013). The other three *FRO* genes in the cucumber genome have not been previously characterized. *FRO3* and *FRO4* were not elevated over control in any of the treatments, suggesting that they are not regulated by Fe or Cu status. However, *FRO2* was upregulated in the -Fe-Cu treatment, but not in the -Fe+Cu treatments, demonstrating that *FRO2* is regulated by Cu status. This gene is also most closely related to Arabidopsis *FRO4* and *FRO5* (Fig. 5c), which are Cu regulated Cu(II) reductases involved in Cu uptake (Bernal *et al.*, 2012).

Transcriptomic characterization of Fe and Cu regulated genes

Since Fe homeostasis is disrupted in the *fefe* mutant and the *fefe* phenotype is rescued by Cu deficiency, we next performed RNA-seq transcriptome analysis of *fefe* and WT roots under control (+Fe, +Cu) conditions and Fe and Cu deficiency. To determine Fe deficiency differentially expressed genes, we used the *fefe* mutant and two WT lines, Edisto and snake melon. The total number of Fe deficiency upregulated genes (1333) combined from all three genotypes (Fig. 6) exceeded the number of downregulated genes (368). 91% of upregulated genes and 98% of the Fe deficiency downregulated genes had differential expression in roots of only one genotype, similar to a previous microarray study with three accessions of Arabidopsis (Stein & Waters, 2012). Of Fe deficiency upregulated genes (Fig. 6a), none were upregulated in all three genotypes, and 7 and 25 were upregulated in *fefe* and Edisto, and *fefe* and snake melon roots, respectively (Table S2). 82 genes were upregulated in the two wild types but not in *fefe* (Table S3). These genes reflect loss of regulation in *fefe* and likely include most or all of the *fefe* regulated transcriptome. The genes that were upregulated by Fe deficiency in only one genotype are shown in Table S4. Of the Fe deficiency downregulated genes (Fig. 6b), none were down in roots of all three genotypes, while 2 and 4 were downregulated in *fefe* and Edisto, and *fefe* and snake melon, respectively, and 3 that were downregulated in both WTs (Table S5). Genes that were downregulated in Fe deficient roots in only one genotype are shown in Table S6. We also

noted that many genes that were upregulated in one or both of the two WTs were significantly downregulated in *fefe* (Fig. 6c). This opposite regulation pattern was present for 5 genes that were upregulated in both WTs, and for 25 and 5 that were upregulated in snake melon and Edisto, respectively (Table S7). For the other opposite expression pattern, genes upregulated in *fefe* and downregulated in the wildtypes (Fig. 6d), one gene was downregulated for both WTs and upregulated in *fefe*, and 3 and 6 were downregulated in snake melon and Edisto, respectively (Table S7).

We also used RNA-seq to quantify changes in root transcript abundance in *fefe* and the WT Edisto in response to 9 d of Cu deficiency (Fig. 7). In common to both WT and *fefe*, 147 genes were upregulated and 63 were downregulated (Table S8). Of Cu deficiency regulated genes, 16.6% had the same expression pattern in both mutant and WT, which was substantially greater than the 1.5% of Fe regulated genes that were in common between *fefe* and Edisto specifically (Fig. 6), suggesting that the root Cu transcriptome is not as drastically affected by the *fefe* mutation as the root Fe transcriptome. Additionally, only 5 genes had opposite regulation patterns (e.g. upregulated in one genotype and downregulated in the other) under Cu deficiency (Table S8). Supplementary table are presented for genes that were upregulated (Table S9) or downregulated (Table S10) in only one genotype.

We next compared the Fe and Cu deficiency differentially expressed genes to determine which genes were regulated by both metals in roots (Fig. 8). We identified 83 genes of 1312 (6.3%) that were upregulated by both Fe and Cu in various combinations (Fig. 8a, Table S11). 29 of 677 genes (4.2%) were downregulated by Fe and/or Cu deficiency in either or both *fefe* and Edisto (Fig. 8b, Table S12). To determine potential effects of Fe and Cu deficiencies on metal homeostasis, we focused on genes from known metal-related gene families. Cucumber coding sequence annotations from the ICuGI database, based on the closest *Arabidopsis thaliana* BLAST hit, were organized by gene family. Normalized read counts for each significantly upregulated or downregulated gene are presented in Table 1. Notably, several genes of the classical Strategy I Fe deficiency response (orthologs of *FRO2*, *IRT1*, *Nramp1*, and *FIT*) were upregulated in one or both WTs, but were not upregulated or were downregulated in *fefe*. Of note, the *IRT* gene in melon that was most orthologous to AtIRT1 function was most homologous to Arabidopsis *AtIRT2* sequence.

Synergy between Fe and Cu regulation of Fe uptake genes

We next examined Fe and Cu regulation of root ferric-chelate reductase activity and used real-time RT-PCR to measure expression of the melon *IRT1*, *FRO1*, *FRO2*, *FIT*, *Nramp1*, and *COPT2* genes to determine whether the combination of Fe and Cu deficiencies acted synergistically. WT and *fefe* plants grown on control (+Fe+Cu) solution had low ferric-chelate reductase activity (Fig. 9a), and baseline gene expression (Fig. 9b–g). As before, *fefe* roots did not increase ferric-chelate reductase activity under -Fe+Cu conditions, and did not have elevated *FRO1* expression, while WT roots had high ferric-chelate reductase activity and high expression of *FRO1*. Under the +Fe-Cu treatment, ferric-chelate reductase activity was elevated in both *fefe* and WT, and *FRO2* expression was increased in both *fefe* and WT roots, similar to the cucumber results (Fig. 5). *FIT* expression increased in both genotypes under -Fe+Cu treatment but not in the +Fe-Cu treatment (Fig. 9b), suggesting that FRO2

expression was responsible for most of the ferric-chelate reductase activity in Cu deficient roots in a FIT-independent manner. This also suggested that fefe roots can sometimes increase *FIT* expression, but this alone is not enough to induce *FRO1* (Fig. 9c) or root ferric chelate reductase activity. Ferric-chelate reductase activity was highly elevated under the simultaneous -Fe-Cu treatment in both WT and *fefe*, and *FIT* and *FRO1* expression were elevated in *fefe*. Both WT and *fefe* also had upregulated *FRO2* expression in the -Fe-Cu treatment. These results show that *fefe* is unable to upregulate *FRO1* normally, that is, under Fe deficiency, but can upregulate *FRO1* under simultaneous Fe and Cu deficiency. Also, these results demonstrate that *FRO2* is a Cu regulated gene that encodes a protein with ferric-chelate reductase activity, and is regulated by Cu. *IRT1* was slightly (~2-fold) upregulated in the +Fe-Cu and -Fe+Cu treatments (Fig. 9e), and more highly under simultaneous Fe and Cu deficiency, especially in *fefe*. *Nramp1* was upregulated only in WT roots by Fe deficiency (Fig. 9f), and only in *fefe* by simultaneous Fe and Cu deficiency. *COPT2* was upregulated in both genotypes in response to both Fe deficiency, and responded strongly to simultaneous Fe and Cu deficiencies (Fig. 9g).

Discussion

The overall objective of this study was to use the *fefe* mutant as a tool to increase understanding of Fe uptake regulation and how Fe–Cu crosstalk influences Fe uptake regulation. Here, we showed that the *fefe* lesion is specific to roots and *FeFe* is required for normal expression of Fe uptake genes, but is not homologous to *FIT*. Thus, *fefe* likely encodes a transcription factor or signaling molecule that functions upstream of *FIT* and Fe uptake gene regulation. We also demonstrated Cu-regulated, *fefe*-independent Fe accumulation, by showing that Cu deficiency stimulates *FRO2* expression and plant Fe accumulation in quantities sufficient to reverse the *fefe* phenotype, but not upregulation of *FIT* or *FRO1*. Simultaneous Fe and Cu deficiencies acted synergistically in the *fefe* mutant to restore ferric-chelate reductase activity and allow expression of *FRO1*.

The *fefe* gene is upstream of Fe uptake genes

We showed that Fe applied to leaves, or increased Fe supply to roots could rescue the *fefe* phenotype (Fig.S1), which suggested that the *fefe* defect results in Fe deficiency specifically. Using grafting, it was clear that *fefe* shoots functioned normally, but the roots did not respond to Fe deficiency (Fig. 3). This indicates that the *fefe* defect does not affect shoot-to-root communication processes (Vert *et al.*, 2003; Garcia *et al.*, 2013), at least at the shoot origin of such a signal, although it is possible that *fefe* roots receive a signal that they are unable to perceive or respond to. Another possibility was that lack of energy resulting from the low photosynthetic capacity of the chlorotic *fefe* leaves rendered it unable to produce or send a root-to-shoot signal. By growing *fefe* plants in conditions to allow green leaves before Fe deficiency treatments, we ruled out this possibility.

The bHLH transcription factors *FER* in tomato (Ling *et al.*, 2002) and *FIT* in Arabidopsis (Colangelo & Guerinot, 2004) are required for upregulation of Fe uptake genes under Fe deficiency. Here, we showed that, like *FER* and *FIT*, the *fefe* mutation also affected expression of Fe uptake genes. In addition, *fefe* did not properly regulate the expression of

melon *FIT* and a number of other genes that were Fe regulated in one or both WT genotypes (Table 1, Figs 2, 9). The upregulation of *FIT* under Fe deficiency was abolished in the *fefe* mutant in Fig. 2 and the RNA-seq experiments (Table 1), but there was some upregulation of *FIT* in Fig. 9. This is similar to Arabidopsis *FIT* expression, where in some experiments *FIT* transcripts are increased under Fe deficiency (Colangelo & Guerinot, 2004; Buckhout *et al.*, 2009; Garcia *et al.*, 2010; Yang *et al.*, 2010), and in others they are not (Dinneny *et al.*, 2008; Long *et al.*, 2010; Ivanov *et al.*, 2012; Stein & Waters, 2012). Regardless, the apparent increased *FIT* expression alone was insufficient to increase *FRO1* (orthologous to *FRO2* in A.t) and *IRT* expression (Fig. 9 and Colangelo & Guerinot, 2004; Yuan *et al.*, 2008). FIT protein activity is not entirely dependent on transcriptional control, as short-lived 'active' forms of FIT protein have been described, and this post-translational control for the protein depends on Fe status (Meiser *et al.*, 2011; Sivitz *et al.*, 2011). Sequencing of the *fefe FIT* locus and RNA-seq sequences of WT and *fefe FIT* transcripts, as well as some level of *FIT* upregulation in *fefe* in Fig. 9 ruled out *FIT* as the mutant gene in *fefe*. Together, these results show that the *fefe* mutant has a defect in regulation of root Fe uptake responses that is upstream of known Fe uptake genes and potentially upstream of or in a partner of *FIT*, making this a valuable mutation for furthering our understanding of Fe uptake regulation. So far, subgroup Ib bHLH transcription factors bHLH038, bHLH039 (Yuan *et al.*, 2008) and bHLH100 and bHLH101 (Wang *et al.*, 2013) have been shown to physically interact with FIT, but single mutants of these genes have no discernable phenotype (Wang *et al.*, 2007; Sivitz *et al.*, 2012; Wang *et al.*, 2013), while the *fefe* phenotype is severe. Thus, it is likely that the *fefe* gene is not homologous to these partner bHLHs, or there is less redundancy in the melon genome for subgroup Ib bHLH genes.

Cu deficiency stimulates Fe uptake

Under Cu deficiency, FeSOD genes and miR398 transcripts are upregulated, and CuSOD genes are downregulated (Yamasaki *et al.*, 2007; Abdel-Ghany & Pilon, 2008; Bernal *et al.*, 2012). We showed an opposite regulatory pattern under Fe deficiency, which led to the Fe/Cu tradeoff hypothesis, that Fe deficiency upregulates Cu accumulation to supply Cu for CuSOD proteins to replace downregulated FeSOD proteins (Waters *et al.*, 2012). Here, we hypothesized that Cu deficiency might stimulate Fe uptake, and the results supported this hypothesis (Fig. 4). We showed that Cu deficiency stimulated the accumulation of Fe in WT and *fefe* plants and rescued the *fefe* phenotype, and also resulted in increased *FRO2* expression and ferric-chelate reductase activity (Figs 5, 9). These results corroborate earlier work that showed Cu deficiency induced ferric-chelate reductase activity (Norvell *et al.*, 1993; Welch *et al.*, 1993; Cohen *et al.*, 1997; Romera *et al.*, 2003), and expands that work by demonstrating Cu regulation of the *FRO2* genes of cucumber and melon (Figs 5, 9, Table 1), which are most closely related to Cu regulated Arabidopsis *FRO4* and *FRO5* genes (Bernal *et al.*, 2012). This is in contrast to regulation of the *FRO1* gene, which was upregulated by Fe deficiency but not Cu deficiency. Since the *fefe* mutant has a root localized defect (Fig. 3) that prevented normal upregulation of *FIT*, *FRO1*, and *IRT1* (Figs 2, 9, Table 1) and normal accumulation of Fe under standard conditions (Figs S1, 1, 4), rescue of this mutant by withholding Cu further supports that Fe uptake is increased under Cu deficiency, consistent with the Fe/Cu tradeoff hypothesis. Cu deficient WT melon plants

also accumulated additional Fe (Fig. 4), showing that this phenomenon is not limited to the *fefe* mutant.

Cu and Fe deficiency effects on metal homeostasis genes

As indicated by differential expression of key metal homeostasis genes (Table 1) under Fe and Cu deficiency, it is clear that deficiency of either Fe or Cu affected overall metal homeostasis. One nicotianamine synthase (*NAS*) gene was downregulated under Fe deficiency, and all three *NAS* genes were downregulated under Cu deficiency. Nicotianamine is an intracellular metal chelator that has been implicated in homeostasis of Fe and Cu (Takahashi *et al.*, 2003; Curie *et al.*, 2009; Klatte *et al.*, 2009). It is not clear if the localization of expression of these three *NAS* genes overlap, or if they are preferentially expressed in certain cell types or organelles. Yellow-stripe-like (*YSL*) and *MATE* genes (e.g. *FRD3*) are potentially involved in intraplant translocation (DiDonato *et al.*, 2004; Green & Rogers, 2004; Waters *et al.*, 2006), and changes in expression of *YSL3* and *MATE* orthologs could result in altered distribution of Fe and Cu under metal deficiency to help plant adaptation to stress. Such redistribution has been observed for Cu and Fe (Ravet *et al.*, 2011; Bernal *et al.*, 2012; Page *et al.*, 2012). Under Cu deficiency, Cu uptake genes *FRO2*, *COPT2*, and *ZIP2* were upregulated, while Fe uptake genes *FRO1* and *IRT1* had decreased expression. This suggests that Fe uptake by Cu deficient melon does not use the primary Fe uptake system, although it is not obvious from the root gene expression data which specific genes could play this role.

Analysis of *fefe* provides new insights into Fe and Cu homeostasis

Gene expression levels in the *fefe* mutant provide new insight into Fe and Cu homeostasis. First, *FRO2* can still be upregulated by Cu deficiency in *fefe* (Fig. 9). Regulation of *FIT* and *FRO1* was defective under Fe deficient conditions (Figs 2, 9, Table 1). Under simultaneous Fe and Cu deficiency, ferric-chelate reductase activity and expression of *FIT*, *FRO1*, *FRO2*, *IRT1*, and *COPT2* were synergistically upregulated in *fefe* (Fig. 9). It is not clear how this synergistic regulation occurs, but high expression of *FIT* in *fefe* suggests that the FIT protein could be involved. One possibility is that a bHLH protein that multimerizes with FIT under Fe deficiency is defective in *fefe*, but an alternative bHLH protein becomes present under Cu deficiency (Fig. 10a) and allows *FIT* expression or activation of FIT and expression of FIT target genes. Several bHLH genes were upregulated in Cu deficient melon roots (Table 1) and some bHLH transcripts were also Cu regulated in Arabidopsis (Yamasaki *et al.*, 2009; Bernal *et al.*, 2012).

Altered transcript abundance (regardless of fold-changes) for metal homeostasis genes in *fefe* (Table 1) indicate potential alterations in cellular metal metabolism. A model of these alterations is shown in Fig. 10, where loss of expression of Fe uptake genes (*FRO1*, *IRT1*, and *Nramp1*) leads to higher expression of *OPT3*, potentially to increase Fe uptake, and higher *NAS1* expression to produce increased nicotianamine. This model also includes altered expression of vacuolar Fe transporters, with the efflux transporter *Nramp3* (Lanquar *et al.*, 2005) more highly expressed, and the influx transporters *VIT1* (Kim *et al.*, 2006) and *NODL* (Gollhofer *et al.*, 2011) at lower abundance, since Fe would be moved out of the vacuole in Fe deficient plants, rather than into the vacuole for storage.

Conclusions and future directions

The Fe/Cu tradeoff hypothesis is that when Fe or Cu is limiting, accumulation of the other metal is stimulated to compensate. This hypothesis was supported by increased Cu accumulation under Fe deficiency (Waters *et al.*, 2012), and results here showed that a *fefe*-independent, Cu-regulated Fe uptake system is present in melon plants. Thus, there are unidentified specific Fe and Cu uptake systems that fulfill this demand, rather than the normal uptake systems acting non-specifically. The *fefe* mutant is a potential tool to identify the Cu-regulated Fe uptake system. The *fefe* mutant could also further understanding of Fe uptake regulation, since the *fefe* protein is likely to be upstream of FIT in the Fe signaling pathway, or works as a partner with the FIT protein. We are actively working to identify the *fefe* gene in melon by positional cloning. The specific mechanism of Fe sensing and signaling of Fe status is unknown, so discovery of the *fefe* gene will facilitate understanding of Fe signaling.

Supplementary Material

Refer to Web version on PubMed Central for supplementary material.

Acknowledgments

The authors thank Grace Troupe and Colin Nogowski for technical assistance, and Raghuprakash Kastoori Ramamurthy for critical reading of the manuscript. This work was supported in part by a USDA-NIFA grant (2014-67013-21658) to B.M.W. The University of Nebraska Medical Center DNA Sequencing Core receives partial support from the NCRR (1S10RR027754-01, 5P20RR016469, RR018788-08) and the National Institute for General Medical Science (NIGMS, 8P20GM103427, GM103471-09). This publication's contents are the sole responsibility of the authors and do not necessarily represent the official views of the NIH or NIGMS.

References

Abdel-Ghany SE, Pilon M. MicroRNA-mediated systemic down-regulation of copper protein expression in response to low copper availability in Arabidopsis. Journal of Biological Chemistry. 2008; 283:15932–15945. [PubMed: 18408011]

Alscher RG, Erturk N, Heath LS. Role of superoxide dismutases (SODs) in controlling oxidative stress in plants. Journal of Experimental Botany. 2002; 53:1331–1341. [PubMed: 11997379]

Benjamini Y, Hochberg Y. Controlling the false discovery rate: a practical and powerful approach to multiple testing. Journal of the Royal Statistical Society. Series B (Methodological). 1995; 57:289–300.

Bernal M, Casero D, Singh V, Wilson GT, Grande A, Yang H, Dodani SC, Pellegrini M, Huijser P, Connolly EL, et al. Transcriptome sequencing identifies SPL7-regulated copper acquisition genes FRO4/FRO5 and the copper dependence of iron homeostasis in Arabidopsis. The Plant Cell. 2012; 24:738–761. [PubMed: 22374396]

Buckhout TJ, Yang TJW, Schmidt W. Early iron-deficiency-induced transcriptional changes in Arabidopsis roots as revealed by microarray analyses. BMC Genomics. 2009; 10:147. [PubMed: 19348669]

Burkhead JL, Reynolds KAG, Abdel-Ghany SE, Cohu CM, Pilon M. Copper homeostasis. New Phytologist. 2009; 182:799–816. [PubMed: 19402880]

Chaignon V, Di Malta D, Hinsinger P. Fe-deficiency increases Cu acquisition by wheat cropped in a Cu-contaminated vineyard soil. New Phytologist. 2002; 154:121–130.

Chen YX, Shi JY, Tian GM, Zheng SJ, Lin Q. Fe deficiency induces Cu uptake and accumulation in Commelina communis. Plant Science. 2004; 166:1371–1377.

Cohen CK, Norvell WA, Kochian LV. Induction of the root cell plasma membrane ferric reductase. An exclusive role for Fe and Cu. Plant Physiology. 1997; 114:1061–1069.

Colangelo EP, Guerinot ML. The essential basic helix-loop-helix protein FIT1 is required for the iron deficiency response. The Plant Cell. 2004; 16:3400–3412. [PubMed: 15539473]

Curie C, Cassin G, Couch D, Divol F, Higuchi K, Jean M, Misson J, Schikora A, Czernic P, Mari S. Metal movement within the plant: contribution of nicotianamine and yellow stripe 1-like transporters. Annals of Botany. 2009; 103:1–11. [PubMed: 18977764]

del Pozo T, Cambiazo V, González M. Gene expression profiling analysis of copper homeostasis in Arabidopsis thaliana. Biochemical and Biophysical Research Communications. 2010; 393:248–252. [PubMed: 20117084]

DiDonato RJ Jr. Roberts LA, Sanderson T, Eisley RB, Walker EL. Arabidopsis Yellow Stripe-Like2 (YSL2): a metal-regulated gene encoding a plasma membrane transporter of nicotianamine-metal complexes. Plant Journal. 2004; 39:403–414. [PubMed: 15255869]

Dinneny JR, Long TA, Wang JY, Jung JW, Mace D, Pointer S, Barron C, Brady SM, Schiefelbein J, Benfey PN. Cell identity mediates the response of Arabidopsis roots to abiotic stress. Science. 2008; 320:942–945. [PubMed: 18436742]

Garcia MJ, Lucena C, Romera FJ, Alcantara E, Perez-Vicente R. Ethylene and nitric oxide involvement in the up-regulation of key genes related to iron acquisition and homeostasis in Arabidopsis. Journal of Experimental Botany. 2010; 61:3885–3899. [PubMed: 20627899]

Garcia MJ, Romera FJ, Stacey MG, Stacey G, Villar E, Alcantara E, Perez-Vicente R. Shoot to root communication is necessary to control the expression of iron-acquisition genes in Strategy I plants. Planta. 2013; 237:65–75. [PubMed: 22983673]

Gayomba SR, Jung H-i, Yan J, Danku J, Rutzke MR, Bernal M, Kramer U, Kochian L, Salt D, Vatamaniuk OK. The CTR/COPT-dependent copper uptake and SPL7-dependent copper deficiency responses are required for basal cadmium tolerance in A. thaliana. Metallomics. 2013; 5:1262. [PubMed: 23835944]

Gollhofer J, Schläwicke C, Jungnick N, Schmidt W, Buckhout TJ. Members of a small family of nodulin-like genes are regulated under iron deficiency in roots of Arabidopsis thaliana. Plant Physiology and Biochemistry. 2011; 49:557–564. [PubMed: 21411332]

González V, Rodríguez-Moreno L, Centeno E, Benjak A, Garcia-Mas J, Puigdomènech P, Aranda M. Genome-wide BAC-end sequencing of Cucumis melo using two BAC libraries. BMC Genomics. 2010; 11:1–11. [PubMed: 20044946]

Green LS, Rogers EE. FRD3 controls iron localization in Arabidopsis. Plant Physiology. 2004; 136:2523–2531. [PubMed: 15310833]

Halliwell B, Gutteridge JMC. Biologically relevant metal ion-dependent hydroxyl radical generation. FEBS Letters. 1992; 307:108–112. [PubMed: 1322323]

Hansch R, Mendel RR. Physiological functions of mineral micronutrients (Cu, Zn, Mn, Fe, Ni, Mo, B, Cl). Current Opinion in Plant Biology. 2009; 12:259–266. [PubMed: 19524482]

Huang S, Li R, Zhang Z, Li L, Gu X, Fan W, Lucas W, Wang X, Xie B, Ni P, et al. The genome of the cucumber, Cucumis sativus L. Nature Genetics. 2009; 41:1275–1283. [PubMed: 19881527]

Ivanov R, Brumbarova T, Bauer P. Fitting into the harsh reality: regulation of iron-deficiency responses in dicotyledonous plants. Molecular Plant. 2012; 5:27–42. [PubMed: 21873619]

Jakoby M, Wang HY, Reidt W, Weisshaar B, Bauer P. FRU (BHLH029) is required for induction of iron mobilization genes in Arabidopsis thaliana. FEBS Letters. 2004; 577:528–534. [PubMed: 15556641]

Jolley VD, Brown JC, Nugent PE. A genetically related response to iron deficiency stress in muskmelon. Plant and Soil. 1991; 130:87–92.

Kim SA, Punshon T, Lanzirotti A, Li LT, Alonso JM, Ecker JR, Kaplan J, Guerinot ML. Localization of iron in Arabidopsis seed requires the vacuolar membrane transporter VIT1. Science. 2006; 314:1295–1298. [PubMed: 17082420]

Klatte M, Schuler M, Wirtz M, Fink-Straube C, Hell R, Bauer P. The analysis of Arabidopsis nicotianamine synthase mutants reveals functions for nicotianamine in seed iron loading and iron deficiency responses. Plant Physiology. 2009; 150:257–271. [PubMed: 19304929]

Kliebenstein DJ, Monde R-A, Last RL. Superoxide dismutase in Arabidopsis: an eclectic enzyme family with disparate regulation and protein localization. Plant Physiology. 1998; 118:637–650. [PubMed: 9765550]

Kurepa J, Bueno P, Kampfenkel K, VanMontagu M, VandenBulcke M, Inze D. Effects of iron deficiency on iron superoxide dismutase expression in Nicotiana tabacum. Plant Physiology and Biochemistry. 1997; 35:467–474.

Langmead B, Salzberg SL. Fast gapped-read alignment with Bowtie 2. Nature Methods. 2012; 9:357–U354. [PubMed: 22388286]

Lanquar V, Lelièvre F, Bolte S, Hamès C, Alcon C, Neumann D, Vansuyt G, Curie C, Schröder A, Krämer U, et al. Mobilization of vacuolar iron by AtNRAMP3 and AtNRAMP4 is essential for seed germination on low iron. Embo Journal. 2005; 24:4041–4051. [PubMed: 16270029]

Ling HQ, Bauer P, Bereczky Z, Keller B, Ganal M. The tomato fer gene encoding a bHLH protein controls iron-uptake responses in roots. Proceedings of the National Academy of Sciences, USA. 2002; 99:13938–13943.

Livak KJ, Schmittgen TD. Analysis of relative gene expression data using real-time quantitative PCR and the 2(-Delta Delta C(T)) method. Methods. 2001; 25:402–408. [PubMed: 11846609]

Long TA, Tsukagoshi H, Busch W, Lahner B, Salt DE, Benfey PN. The bHLH transcription factor POPEYE regulates response to iron deficiency in Arabidopsis roots. The Plant Cell. 2010; 22:2219–2236. [PubMed: 20675571]

Meiser J, Lingam S, Bauer P. Posttranslational regulation of the iron deficiency basic helix-loop-helix transcription factor FIT is affected by iron and nitric oxide. Plant Physiology. 2011; 157:2154–2166. [PubMed: 21972265]

Mukherjee I, Campbell NH, Ash JS, Connolly EL. Expression profiling of the Arabidopsis ferric chelate reductase (FRO) gene family reveals differential regulation by iron and copper. Planta. 2006; 223:1178–1190. [PubMed: 16362328]

Myouga F, Hosoda C, Umezawa T, Iizumi H, Kuromori T, Motohashi R, Shono Y, Nagata N, Ikeuchi M, Shinozaki K. A heterocomplex of iron superoxide dismutases defends chloroplast nucleoids against oxidative stress and is essential for chloroplast development in Arabidopsis. The Plant Cell Online. 2008; 20:3148–3162.

Norvell WA, Welch RM, Adams ML, Kchian LV. Reduction of Fe(III), Mn(III) and Cu(II) chelates by roots of pea (Pisum sativum L.) or soybean (Glycine max). Plant and Soil. 1993; 156:123–126.

Nugent P. Iron chlorotic melon germplasm C940-fe. Hortscience. 1994; 29:50–51.

Nugent PE, Bhella H. A new chlorotic mutant of muskmelon. Hortscience. 1988; 23:379–381.

Page MD, Allen MD, Kropat J, Urzica EI, Karpowicz SJ, Hsieh SI, Loo JA, Merchant SS. Fe sparing and Fe recycling contribute to increased superoxide dismutase capacity in iron-starved Chlamydomonas reinhardtii. The Plant Cell. 2012; 24:2649–2665. [PubMed: 22685165]

Paolacci AR, Celletti S, Catarcione G, Hawkesford MJ, Astolfi S, Ciaffi M. Iron deprivation results in a rapid but not sustained increase of the expression of genes involved in iron metabolism and sulfate uptake in tomato (Solanum lycopersicum L.) seedlings. Journal of Integrative Plant Biology. 2013; 56:88–100. [PubMed: 24119307]

Perea-García A, Garcia-Molina A, Andrés-Colás N, Vera-Sirera F, Pérez-Amador MA, Puig S, Peñarrubia L. Arabidopsis copper transport protein COPT2 participates in the cross talk between iron deficiency responses and low-phosphate signaling. Plant Physiology. 2013; 162:180–194. [PubMed: 23487432]

Pilon M, Ravet K, Tapken W. The biogenesis and physiological function of chloroplast superoxide dismutases. Biochimica Et Biophysica Acta-Bioenergetics. 2011; 1807:989–998.

Pineau C, Loubet S, Lefoulon C, Chalies C, Fizames C, Lacombe B, Ferrand M, Loudet O, Berthomieu P, Richard O. Natural variation at the FRD3 MATE transporter locus reveals cross-talk between Fe homeostasis and Zn tolerance in Arabidopsis thaliana. PLoS Genetics. 2012; 8:e1003120. [PubMed: 23236296]

Puig S, Andres-Colas N, Garcia-Molina A, Penarrubia L. Copper and iron homeostasis in Arabidopsis: responses to metal deficiencies, interactions and biotechnological applications. Plant, Cell and Environment. 2007; 30:271–290.

Ravet K, Danford FL, Dihle A, Pittarello M, Pilon M. Spatiotemporal analysis of copper homeostasis in Populus trichocarpa reveals an integrated molecular remodeling for a preferential allocation of copper to plastocyanin in the chloroplasts of developing leaves. Plant Physiology. 2011; 157:1300–1312. [PubMed: 21941002]

Robinson MD, McCarthy DJ, Smyth GK. edgeR: a bioconductor package for differential expression analysis of digital gene expression data. Bioinformatics. 2010; 26:139–140. [PubMed: 19910308]

Romera FJ, Frejo VM, Alcántara E. Simultaneous Fe- and Cu-deficiency synergically accelerates the induction of several Fe-deficiency stress responses in Strategy I plants. Plant Physiology and Biochemistry. 2003; 41:821–827.

Sancenon V, Puig S, Mira H, Thiele DJ, Penarrubia L. Identification of a copper transporter family in Arabidopsis thaliana. Plant Molecular Biology. 2003; 51:577–587. [PubMed: 12650623]

Sivitz A, Grinvalds C, Barberon M, Curie C, Vert G. Proteasome-mediated turnover of the transcriptional activator FIT is required for plant irondeficiency responses. The Plant Journal. 2011; 66:1044–1052. [PubMed: 21426424]

Sivitz AB, Hermand V, Curie C, Vert G. Arabidopsis bHLH100 and bHLH101 control iron homeostasis via a FIT-independent pathway. PloS one. 2012; 7:e44843. [PubMed: 22984573]

Stein RJ, Waters BM. Use of natural variation reveals core genes in the transcriptome of iron-deficient Arabidopsis thaliana roots. Journal of Experimental Botany. 2012; 63:1039–1055. [PubMed: 22039296]

Takahashi M, Terada Y, Nakai I, Nakanishi H, Yoshimura E, Mori S, Nishizawa M. Role of nicotianamine in the intracellular delivery of metals and plant reproductive development. Plant Cell. 2003; 15:1263–1280. [PubMed: 12782722]

Vert GA, Briat JF, Curie C. Dual regulation of the Arabidopsis high-affinity root iron uptake system by local and long-distance signals. Plant Physiology. 2003; 132:796–804. [PubMed: 12805609]

von Wiren N, Gazzarrini S, Gojont A, Frommer WB. The molecular physiology of ammonium uptake and retrieval. Current Opinion in Plant Biology. 2000; 3:254–261. [PubMed: 10837267]

Wang HY, Klatte M, Jakoby M, Baumlein H, Weisshaar B, Bauer P. Iron deficiency-mediated stress regulation of four subgroup Ib BHLH genes in Arabidopsis thaliana. Planta. 2007; 226:897–908. [PubMed: 17516080]

Wang N, Cui Y, Liu Y, Fan H, Du J, Huang Z, Yuan Y, Wu H, Ling H-Q. Requirement and functional redundancy of Ib subgroup bHLH proteins for iron deficiency responses and uptake in Arabidopsis thaliana. Molecular plant. 2013; 6:503–513. [PubMed: 22983953]

Wang Y-H, Garvin DF, Kochian LV. Rapid induction of regulatory and transporter genes in response to phosphorus, potassium, and iron deficiencies in tomato roots. Evidence for cross talk and root/rhizospheremediated signals. Plant Physiology. 2002; 130:1361–1370. [PubMed: 12428001]

Waters BM, Armbrust LC. Optimal copper supply is required for normal plant iron deficiency responses. Plant Signaling & Behavior. 2013; 8:e26611. [PubMed: 24084753]

Waters BM, Blevins DG, Eide DJ. Characterization of FRO1, a pea ferricchelate reductase involved in root iron acquisition. Plant Physiology. 2002; 129:85–94. [PubMed: 12011340]

Waters BM, Chu HH, DiDonato RJ, Roberts LA, Eisley RB, Lahner B, Salt DE, Walker EL. Mutations in Arabidopsis Yellow Stripe-Like1 and Yellow Stripe-Like3 reveal their roles in metal ion homeostasis and loading of metal ions in seeds. Plant Physiology. 2006; 141:1446–1458. [PubMed: 16815956]

Waters BM, Lucena C, Romera FJ, Jester GG, Wynn AN, Rojas CL, Alcantara E, Perez-Vicente R. Ethylene involvement in the regulation of the H+- ATPase CsHA1 gene and of the new isolated ferric reductase CsFRO1 and iron transporter CsIRT1 genes in cucumber plants. Plant Physiology and Biochemistry. 2007; 45:293–301. [PubMed: 17468001]

Waters BM, McInturf SA, Stein RJ. Rosette iron deficiency transcript and microRNA profiling reveals links between copper and iron homeostasis in Arabidopsis thaliana. Journal of Experimental Botany. 2012; 63:5903–5918. [PubMed: 22962679]

Waters BM, Troupe GC. Natural variation in iron use efficiency and mineral remobilization in cucumber (Cucumis sativus). Plant and Soil. 2012; 352:185–197.

Welch RM, Norvell WA, Schaefer SC, Shaff JE, Kochian LV. Induction of iron(III) and copper(II) reduction in pea (Pisum sativum L.) roots by Fe and Cu staus: Does the root-cell plasmalemma

Fe(III)-chelate reductase perform a general role in regulating cation uptake? Planta. 1993; 1993:555–561.

Wintz H, Fox T, Wu YY, Feng V, Chen WQ, Chang HS, Zhu T, Vulpe C. Expression profiles of Arabidopsis thaliana in mineral deficiencies reveal novel transporters involved in metal homeostasis. Journal of Biological Chemistry. 2003; 278:47644–47653. [PubMed: 13129917]

Yamasaki H, Abdel-Ghany SE, Cohu CM, Kobayashi Y, Shikanai T, Pilon M. Regulation of copper homeostasis by micro-RNA in Arabidopsis. Journal of Biological Chemistry. 2007; 282:16369–16378. [PubMed: 17405879]

Yamasaki H, Hayashi M, Fukazawa M, Kobayashi Y, Shikanai T. SQUAMOSA promoter binding protein-like7 is a central regulator for copper homeostasis in Arabidopsis. The Plant Cell. 2009; 21:347–361. [PubMed: 19122104]

Yang TJW, Lin W-D, Schmidt W. Transcriptional profiling of the Arabidopsis iron deficiency response reveals conserved transition metal homeostasis networks. Plant Physiology. 2010; 152:2130–2141. [PubMed: 20181752]

Yuan YX, Wu HL, Wang N, Li J, Zhao WN, Du J, Wang DW, Ling HQ. FIT interacts with AtbHLH38 and AtbHLH39 in regulating iron uptake gene expression for iron homeostasis in Arabidopsis. Cell Research. 2008; 18:385–397. [PubMed: 18268542]

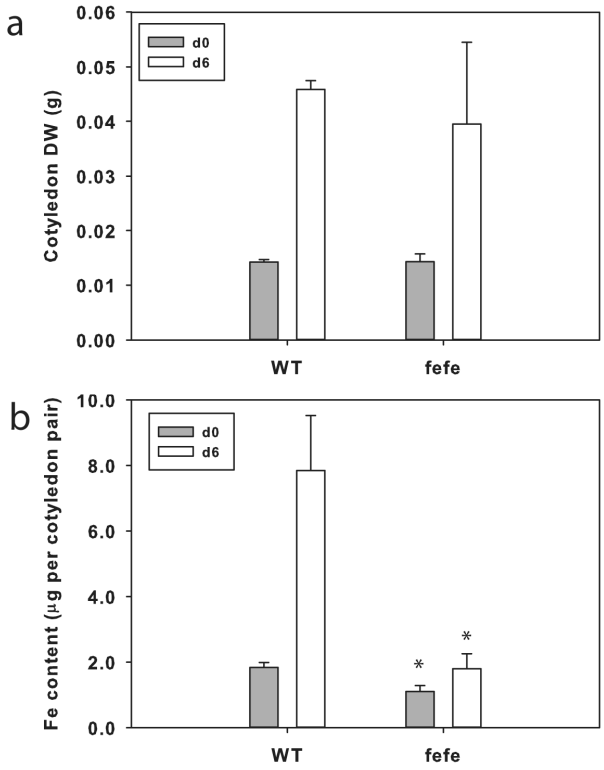

Fig. 1.

Accumulation of iron (Fe) during seedling early growth of *Cucumis melo*. (a) Dry weight (DW) of wild type (WT) and *fefe* mutant cotyledon pairs (± SD) at planting (d0, closed bars) and after 6 d growth on complete nutrient solution (10 µM Fe, 0.5 µM Cu; open bars). (b) Fe content of cotyledon pairs (± SD) of WT and *fefe* mutant cotyledons at planting (d0; closed bars) and after 6 d growth (open bars) on complete solution. Significant difference between WT and *fefe*: *, $P<0.05$.

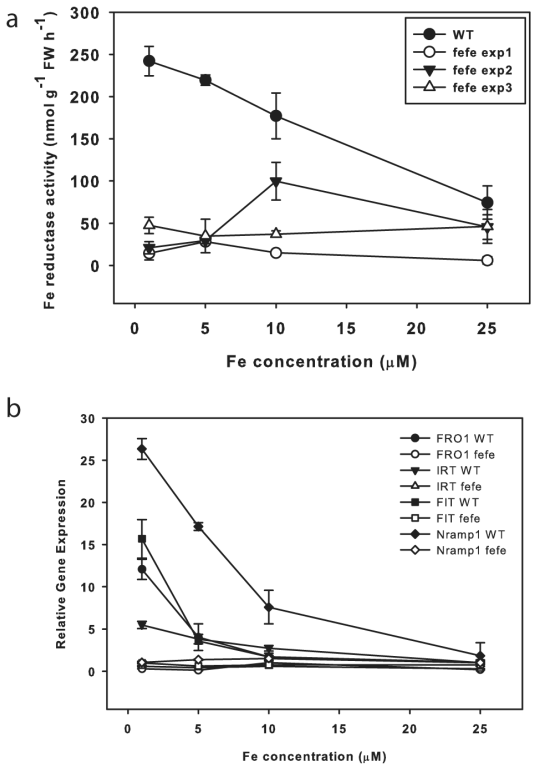

Fig. 2.

The *fefe* mutant of *Cucumis melo* does not upregulate iron (Fe) uptake genes. (a) Root ferric-chelate reductase activity (± SD) after 3 d of treatment. Figure shows a representative experiment of wild type (WT) and three separate experiments of *fefe* roots over a range of Fe concentrations. (b) Quantitative real-time RT-PCR for *FRO1*, *FIT*, *Nramp1*, and *IRT1* in WT and *fefe* mutant roots. Relative expression as normalized to ubiquitin and WT at 25 μM Fe.

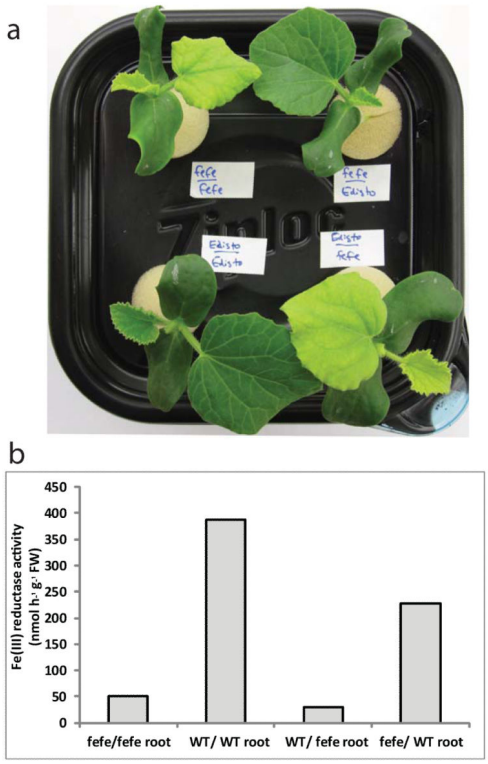

Fig. 3.

The *fefe* defect is localized to the roots of *Cucumis melo* as determined by grafting. (a) Shoot phenotype of grafted plants. Upper left, *fefe* scion grafted to *fefe* rootstock, upper right, *fefe* scion grafted to WT (Edisto) rootstock, lower left, wild type (WT) scion grafted to WT rootstock, lower right, WT scion grafted to *fefe* rootstock. (b) Root ferric-chelate reductase activity after transferring individual plants shown in (a) to -Fe solution for 3 d. *x*-axis indicates scion first and rootstock second.

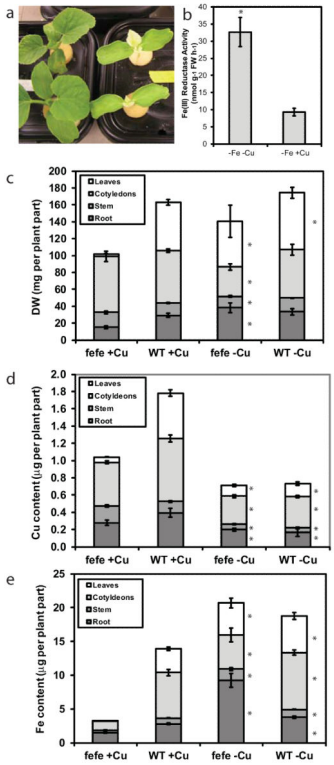

Fig. 4.

Copper (Cu) deficiency of *Cucumis melo* stimulates iron (Fe) uptake and rescues the *fefe* phenotype. (a) Photograph of *fefe* plants grown without Cu (left) and on complete nutrient solution (right). (b) Root ferric-chelate reductase activity (± SD) after transferring rescued *fefe* plants to -Fe-Cu or -Fe+Cu solution for 3 d. (c–e) Stacked bar graphs of (c) dry weight (DW), (d) Cu content, and (e) Fe content of plant parts for *fefe* and wild type (WT) plants (± SE) grown with or without Cu. Significant difference between +Cu and -Cu treatments: *, $P<0.05$.

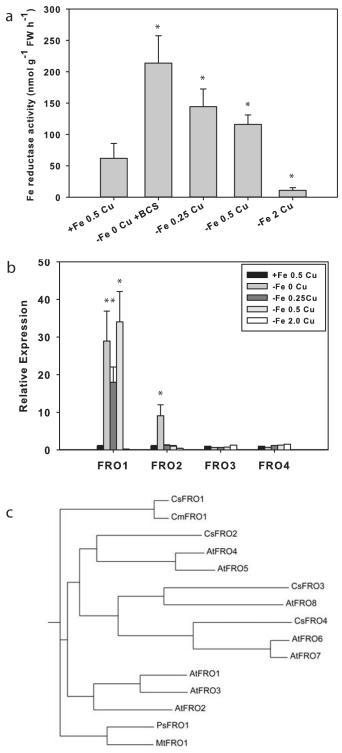

Fig. 5.

Iron (Fe) and copper (Cu) regulation of cucumber (*Cucumis sativus*) *FRO* genes. (a) Root ferric-chelate reductase activity (± SD) after 3 d of treatment for control (+Fe, 0.5 μM Cu) and -Fe with a range of Cu supply. (b) Quantitative real-time RT-PCR of expression (± SD) of four cucumber *FRO* genes from the plants in (a). Significant difference between control and treatments: *, $P<0.05$. (c) Phylogenetic tree drawn from ClustalW alignment of FRO protein sequences from cucumber (Cs), melon (Cm), Arabidopsis (At), *Pisum sativum* (Ps), and *Medicago truncatula* (Mt).

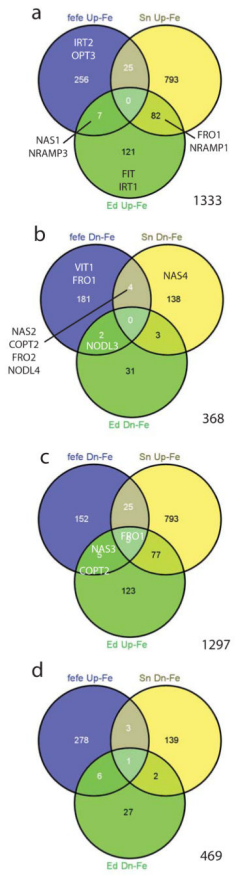

Fig. 6.

Venn diagrams for iron (Fe) regulated genes in *fefe* and two wild-type (WT) *Cucumis melo* accessions, Edisto (Ed) and snake melon (sn). Genes of interest are shown in the appropriate set or overlap of sets. (a) Genes upregulated under Fe deficiency, (b) genes downregulated under Fe deficiency, (c) genes downregulated in *fefe* and upregulated in WTs, (d) genes upregulated in *fefe* and downregulated in WTs.

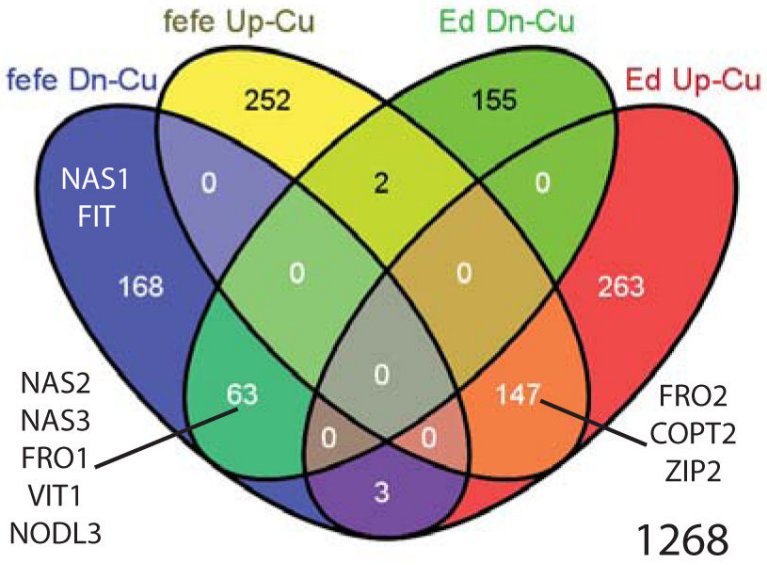

Fig. 7.

Venn diagram of genes upregulated (Up) or downregulated (Dn) under copper (Cu) deficiency in *fefe* or wild type (WT) Edisto (Ed) *Cucumis melo* roots. Genes of interest are shown in the appropriate set or overlap of sets.

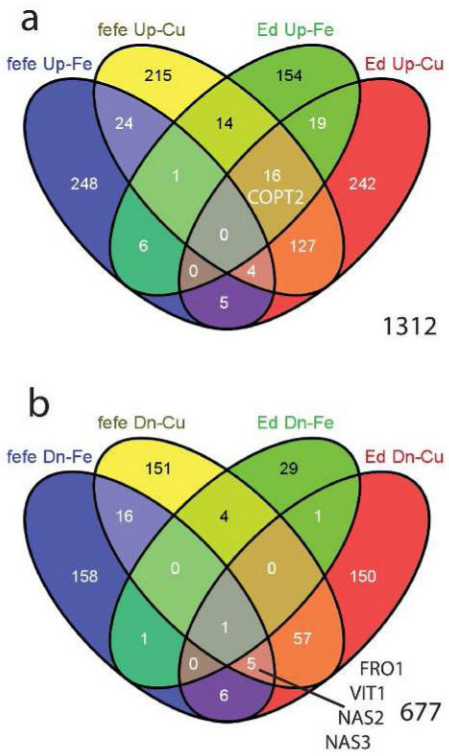

Fig. 8.

Venn diagrams to identify number of overlapping genes in iron (Fe) and copper (Cu) regulated genes of *Cucumis melo* roots. (a) Genes upregulated in *fefe* and Edisto (Ed) under Fe deficiency and/or Cu deficiency, (b) genes downregulated in *fefe* and Edisto (Ed) under Fe deficiency and/or Cu deficiency. Genes of interest are shown in the appropriate set or overlap of sets.

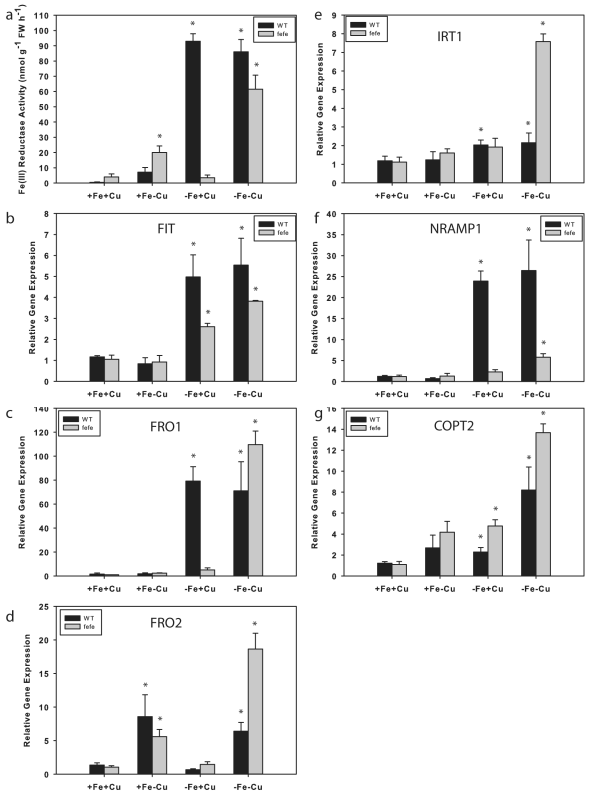

Fig. 9.

Regulation of melon (*Cucumis melo*) root ferric-chelate reductase activity and iron (Fe) uptake gene expression by Fe and copper (Cu). (a) Ferric-chelate reductase activity (± SD) in roots after 3 d treatment with 10 μM Fe and 0.5 μM Cu (+Fe+Cu), -Fe+Cu, +Fe-Cu, or -Fe-Cu solutions. Wild type (WT), black bars; *fefe* mutant, grey bars. Gene expression in roots of the plants above, for (b) *FIT*, (c) *FRO1*, (d) *FRO2*, (e) *IRT1*, (f) *NRAMP1*, and (g) *COPT2*. Significant difference between control (+Fe+Cu) and treatments: *, $P<0.05$.

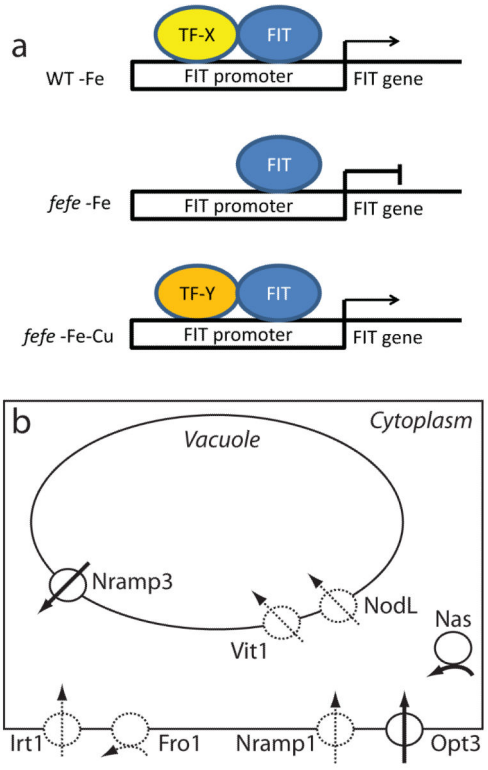

Fig. 10.

Models of effects of the *fefe* mutation of *Cucumis melo*. (a) Model of potential *FIT* regulation under single iron (Fe) or copper (Cu) deficiencies, or simultaneous Fe and Cu deficiency. In wild type (WT), FIT upregulates its own expression with a required partner bHLH protein, which is missing or mutated in *fefe*. A substitute partner protein is upregulated by Cu deficiency, which allows the *fefe* mutant to transcribe *FIT* and activate FIT targets. (b) Model of metal homeostasis alterations in *fefe* roots based on transcript abundance. Dashed lines represent lower expression relative to WT, solid lines represent higher expression relative to WT. Transport of Fe into a generic cell is represented for Fro1, Irt1, Nramp1, and Opt3 proteins, transport of Fe into the vacuole is represented by Vit1 and NodL proteins, transport out of a vacuole is represented by Nramp3 protein, and cytoplasmic synthesis of nicotianamine is represented by Nas protein.

Table 1

Gene expression in wild type (WT) melon (*Cucumis melo*) and *fefe* roots. RNA-seq reads were mapped to cucumber transcripts (Cucumber Locus ID)

			logFC (−Fe/+Fe)			logFC (−Cu/+Cu)		Normalized Read Counts									
								fefe		WT (Edisto)		WT (snake)		*fefe*		WT (Edisto)	
Melon Gene Name	**Cucumber Locus ID**	**Top *Arabidopsis thaliana* Hit**	***fefe***	**WT (Ed)**	**WT (sn)**	***fefe***	**WT (Ed)**	**+Fe**	**−Fe**	**+Fe**	**−Fe**	**+Fe**	**−Fe**	**+Cu**	**−Cu**	**+Cu**	**−Cu**
		Ferric Reductase/oxidase family															
		AT5G47910.1 RBOHD															
Csa3M845500.1	AT5G47910.1 RBOHD (RESPIRATORY BURST OXIDASE HOMOLOGUE D); NAD(P)H oxidase			1.1	1.2	1.7		1346	1976	3650	6671	7516	15847	6058	11256	1066	3005
FRO1	Csa5M175770.1	AT1G23020.1 FRO3; ferric-chelate reductase	-1.7	4.3	2.7	-5.0	-3.3	500	154	410	8058	291	1813	1737	44	1147	123
FRO2	Csa3M183380.1	AT5G23980.1 FRO4 (FERRIC REDUCTION OXIDASE 4); ferric-chelate reductase	-2.1		-2.6	3.8	2.6	2861	663	1004	1678	105	17	201	2424	1894	9337
	Csa1M423270.1	AT2G24520.1 AHA5 (Arabidopsis H(+)-ATPase 5); ATPase		1.1				6572	8012	5025	10303	4560	7387	4229	3279	6239	4469
		Metal Transporters															
Nramp3	Csa2M423700.1	AT2G23150.1 NRAMP3 (NATURAL RESISTANCE-ASSOCIATED MACROPHAGE PROTEIN 3); inorganic anion transmembrane transporter/ manganese ion transmembrane transporter/ metal ion transmembrane transporter	1.1	1.2				6111	13055	1241	2713	1609	2236	2468	1711	994	709
Nramp1	Csa6M382880.1	AT1G80830.1 NRAMP1 (NATURAL RESISTANCE-ASSOCIATED MACROPHAGE PROTEIN 1); inorganic anion transmembrane transporter/ manganese ion transmembrane transporter/ metal ion transmembrane transporter		3.7	1.7			174	84	775	9703	1688	5438	167	89	3078	1280

			logFC (−Fe/+Fe)			logFC (−Cu/+Cu)		Normalized Read Counts									
								fefe		WT (Edisto)		WT (snake)		*fefe*		WT (Edisto)	
Melon Gene Name	**Cucumber Locus ID**	**Top *Arabidopsis thaliana* Hit**	***fefe***	**WT (Ed)**	**WT (sn)**	***fefe***	**WT (Ed)**	**+Fe**	**−Fe**	**+Fe**	**−Fe**	**+Fe**	**−Fe**	**+Cu**	**−Cu**	**+Cu**	**−Cu**
IRT1	Csa1M707110.1	AT4G19680.2 IRT2; iron ion transmembrane transporter/ zinc ion transmembrane transporter		1.4		-2.5		386	248	428	1117	246	473	801	128	614	395
IRT2	Csa6M517980.1	AT4G19690.2 IRT1 (iron-regulated transporter 1); cadmium ion transmembrane transporter/ copper uptake transmembrane transporter/ iron ion transmembrane transporter/ manganese ion transmembrane transporter/ zinc ion transmembrane transporter	3.0					12	103	3	4	6	9	1	1	2	1
ZIP2	Csa7M162550.1	AT5G59520.1 ZIP2; copper ion transmembrane transporter/ transferase, transferring glycosyl groups / zinc ion transmembrane transporter				1.3	2.2	140	72	54	46	78	81	42	85	43	170
ZIP5	Csa4M618490.1	AT1G05300.1 ZIP5; cation transmembrane transporter/ metal ion transmembrane transporter					-1.0	83	81	402	457	173	162	25	31	140	55
COPT2	Csa1M526820.1	AT3G46900.1 COPT2; copper ion transmembrane transporter/ high affinity copper ion transmembrane transporter	-2.5	1.8	-1.6	1.4	1.7	278	49	57	194	47	15	87	184	179	515
	Csa3M696860.1	AT3G08040.1 FRD3 (FERRIC REDUCTASE DEFECTIVE 3); antiporter/ transporter			-3.9	-2.4		65	50	3	19	179	12	20	3	6	14
	Csa7M428170.1	AT3G08040.1 FRD3 (FERRIC REDUCTASE DEFECTIVE 3); antiporter/ transporter		1.3				1425	1322	792	1860	1269	1390	1543	774	2211	1417
	Csa3M180310.1	AT4G23030.1 MATE efflux protein-related		1.0	1.1	1.3	2.8	74	70	158	316	304	620	741	1464	70	423
	Csa2M404760.1	AT1G65730.1 YSL7 (YELLOW STRIPE LIKE 7); oligopeptide transporter			1.0			1129	633	1660	1335	2345	4611	332	333	602	436
	Csa2M404780.1	AT1G48370.1 YSL8 (YELLOW STRIPE LIKE 8); oligopeptide transporter			1.0			71	44	124	108	183	366	27	31	47	43

Melon Gene Name	Cucumber Locus ID	Top *Arabidopsis thaliana* Hit	logFC (−Fe/+Fe)			logFC (−Cu/+Cu)		Normalized Read Counts									
			fefe	WT (Ed)	WT (sn)	*fefe*	WT (Ed)	*fefe*		WT (Edisto)		WT (snake)		*fefe*		WT (Edisto)	
								+Fe	−Fe	+Fe	−Fe	+Fe	−Fe	+Cu	−Cu	+Cu	−Cu
	Csa3M238100.1	AT5G53550.1 YSL3 (YELLOW STRIPE LIKE 3); oligopeptide transporter			-1.2	1.1	1.7	416	289	155	114	318	140	149	272	144	404
	Csa1M329900.1	AT5G53550.1 YSL3 (YELLOW STRIPE LIKE 3); oligopeptide transporter	-1.5					103	37	19	14	37	44	8	14	16	25
OPT3	Csa1M180750.1	AT4G16370.1 ATOPT3 (OLIGOPEPTIDE TRANSPORTER); oligopeptide transporter	2.1					3299	14592	457	872	484	742	1448	740	201	241
		Nicotianamine synthase family															
NAS1	Csa2M034520.1	AT5G04950.1 NAS1 (NICOTIANAMINE SYNTHASE 1); nicotianamine synthase	2.4	2.0		-2.7		5011	2731	21	86	17	9	166	22	42	18
NAS2	Csa1M423010.1	AT1G56430.1 NAS4 (NICOTIANAMINE SYNTHASE 4); nicotianamine synthase	-5.3		-1.4	-5.1	-4.4	139	3	522	210	57	21	80	2	1057	50
NAS3	Csa2M034530.1	AT1G56430.1 NAS4 (NICOTIANAMINE SYNTHASE 4); nicotianamine synthase	-1.8	2.2		-3.5	-3.2	150	44	271	1215	602	469	324	23	520	54
NAS4	Csa1M561410.1	AT1G56430.1 NAS4 (NICOTIANAMINE SYNTHASE 4); nicotianamine synthase			-2.2	-3.3	-1.7	169	81	75	39	80	17	92	8	54	14
		VIT1 family															
VIT1	Csa5M550240.1	AT2G01770.1 VIT1 (vacuolar iron transporter 1); iron ion transmembrane transporter	-3.4			-1.8	-1.3	90	9	567	347	129	131	178	42	244	89
NODL1	Csa1M288020.1	AT4G30420.1 nodulin MtN21 family protein	-1.8		1.1			346	98	1659	2205	1093	2324	104	118	65	36
NODL2	Csa3M835770.1	AT5G40240.1 nodulin MtN21 family protein			1.1			101	135	38	47	41	87	66	79	37	26
NODL3	Csa6M411280.1	AT3G25190.1 nodulin, putative	-4.6	-1.8		-1.4	-1.0	62	3	295	80	124	68	153	48	928	392
NODL4	Csa7M325150.1	AT3G43660.1 nodulin, putative	-2.7		-1.3			35	5	37	27	27	11	31	24	64	64

Melon Gene Name	Cucumber Locus ID	Top *Arabidopsis thaliana* Hit	logFC (−Fe/+Fe)			logFC (−Cu/+Cu)		Normalized Read Counts									
			fefe	WT (Edisto)	WT (snake)	*fefe*	WT (Edisto)	*fefe*		WT (Edisto)		WT (snake)		*fefe*		WT (Edisto)	
								+Fe	−Fe	+Fe	−Fe	+Fe	−Fe	+Cu	−Cu	+Cu	−Cu
Ferritin																	
	Csa5M215130.1	AT2G40300.1 ATFER4 (ferritin 4); binding / ferric iron binding / oxidoreductase/ transition metal ion binding		-1.2				422	320	950	407	817	923	525	371	574	549
	Transcription factors																
	Csa1M074400.1	AT4G20970.1 basic helix-loop-helix (bHLH) family protein	2.6			2.4		69	442	95	186	150	201	65	272	144	243
	Csa1M589140.1	AT5G56960.1 basic helix-loop-helix (bHLH) family protein	1.3		1.2			94	227	212	178	518	1194	15	12	23	10
	Csa2M193320.1	AT5G43650.1 basic helix-loop-helix (bHLH) family protein		1.3	2.2	2.8		12	8	158	387	259	1140	25	148	5	15
	Csa2M354790.1	AT4G33880.1 basic helix-loop-helix (bHLH) family protein/RSL2		4.9	4.5			10	2	2	57	1	23	6	0	3	1
	Csa3M119500.1	AT1G01260.1 basic helix-loop-helix (bHLH) family protein			1.0		1.3	627	676	1342	2432	1569	3072	1573	2262	426	914
	Csa3M178580.1	AT5G51780.1 basix helix-loop-helix (bHLH) family protein			2.0			37	25	10	14	39	155	1	1	1	0
	Csa3M893390.1	AT5G65640.1 bHLH093 (beta HLH protein 93); DNA binding / transcription factor				-1.6	-1.0	594	762	1362	949	3043	2498	114	31	135	56
	Csa4M642470.1	AT2G14760.1 basic helix-loop-helix protein / bHLH protein		1.9				12	8	18	64	0	13	12	6	3	1
	Csa5M420280.1	AT1G66470.1 basic helix-loop-helix (bHLH) family protein			1.1			309	164	66	60	44	89	59	23	46	24
FIT	Csa6M148260.1	AT2G28160.1 FRU (FER-LIKE REGULATOR OF IRON UPTAKE); DNA binding / transcription factor		1.9		-1.1		1045	649	109	404	195	337	809	325	270	187
	Csa6M497100.1	AT2G22750.2 basic helix-loop-helix (bHLH) family protein			1.6			5	4	39	73	142	426	5	18	2	1
	Csa6M497110.1	AT4G37850.1 basic helix-loop-helix (bHLH) family protein			1.8	3.1	2.2	68	30	716	865	428	1413	108	801	21	80

New Phytol. Author manuscript; available in PMC 2015 September 01.

Melon Gene Name	Cucumber Locus ID	Top *Arabidopsis thaliana* Hit	logFC (−Fe/+Fe)			logFC (−Cu/+Cu)		Normalized Read Counts									
								fefe		WT (Edisto)		WT (snake)		*fefe*		WT (Edisto)	
			fefe	WT (Ed)	WT (sn)	*fefe*	WT (Ed)	+Fe	−Fe	+Fe	−Fe	+Fe	−Fe	+Cu	−Cu	+Cu	−Cu
	Csa6M497120.1	AT4G37850.1 basic helix-loop-helix (bHLH) family protein						30	16	5	4	3	11	6	7	5	7
	Csa3M116720.1	AT2G44840.1 ERF13 (ETHYLENE-RESPONSIVE ELEMENT BINDING FACTOR 13); DNA binding / transcription factor			2.4	2.7	3.8	6	2	91	231	120	603	67	345	3	32
	Csa3M116730.1	AT2G44840.1 ERF13 (ETHYLENE-RESPONSIVE ELEMENT BINDING FACTOR 13); DNA binding / transcription factor			2.3	2.1		4	2	31	58	35	164	42	145	2	15
	Csa5M155570.1	AT1G12610.1 DDF1 (DWARF AND DELAYED FLOWERING 1); DNA binding / sequence-specific DNA binding / transcription factor		1.0		2.0	5.0	2	2	292	575	328	340	201	693	2	68
	Csa7M169070.1	AT4G39250.1 ATRL1 (ARABIDOPSIS RAD-LIKE 1); DNA binding / transcription factor		5.0			-6.3	1	1	2	66	10	13	1	0	25	0
	Csa3M180260.1	AT4G25490.1 CBF1 (C-REPEAT/DRE BINDING FACTOR 1); DNA binding / transcription activator/ transcription factor	-1.6	1.1		1.0	3.6	30	9	81	168	153	147	1855	3044	102	1060
	Csa3M710870.1	AT1G80840.1 WRKY40; transcription factor			1.3	1.2	3.4	255	179	1244	2545	2333	5775	3129	5844	248	2303
	Csa7M073700.1	AT4G34410.1 RRTF1 ({REDOX RESPONSIVE TRANSCRIPTION FACTOR 1); DNA binding / transcription factor		1.4	2.1	1.6	4.1	2	2	19	47	21	90	269	670	9	136
	Csa2M297760.1	AT5G50080.1 DNA binding / transcription factor		1.5	1.2			150	96	249	688	169	383	71	32	86	52
	Csa3M405510.1	AT5G48150.1 PAT1 (phytochrome a signal transduction 1); signal transducer/ transcription factor		1.3	1.5		3.6	248	264	558	1349	1442	3993	4608	7412	281	3195
	Csa6M425790.1	AT3G44260.1 CCR4-NOT transcription complex protein,			1.3	1.6	3.0	65	57	269	295	1024	2443	1030	2623	104	701

Melon Gene Name	Cucumber Locus ID	Top *Arabidopsis thaliana* Hit	logFC (−Fe/+Fe)			logFC (−Cu/+Cu)		Normalized Read Counts							
			fefe	WT (Ed)	WT (sn)	*fefe*	WT (Ed)	*fefe*		WT (Edisto)		WT (snake)		*fefe*		WT (Edisto)	
								+Fe	−Fe	+Fe	−Fe	+Fe	−Fe	+Cu	−Cu	+Cu	−Cu
		putative															

Significant log fold-change (logFC) is shown for *fefe*, Edisto (Ed) and snake melon (sn) for Fe treatments, and for Edisto and *fefe* for Cu treatments. Normalized read counts for each transcript are also shown.